Journal of Power Sources 236 (2013) 181–187

Contents lists available at SciVerse ScienceDirect

Journal of Power Sources

journal homepage: www.elsevier.com/locate/jpowsour

Short communication

On the role of polysulfides for a stable solid electrolyte interphase on the lithium anode cycled in lithium–sulfur batteries

Shizhao Xiong*, Kai Xie, Yan Diao, Xiaobin Hong

Department of Material Science and Engineering, College of Aerospace Science and Engineering, National University of Defense Technology, Changsha, Hunan 410073, PR China

HIGHLIGHTS

- ► Polysulfides result in a stable SEI on lithium anode cycled in Li–S batteries.
- ► The SEI formed with polysulfides can be assumed to two sub layers.
- ► The top layer composes of the products of electrolyte solution decomposition.
- ► The bottom layer composes of lithium sulfide produced with polysulfides.
- ► The bottom layer plays an important role to prevent decomposition of LiTFSI.

ARTICLE INFO

Article history:
Received 20 October 2012
Received in revised form
23 February 2013
Accepted 25 February 2013
Available online 5 March 2013

Keywords:
Solid electrolyte interphase
Lithium electrode
Polysulfides
Lithium sulfide
Lithium–sulfur batteries

ABSTRACT

The solid electrolyte interphase on the lithium electrode cycled with an electrolyte solution with polysulfides is investigated by a series of measurement within symmetrical cells. Both discharge–charge curves and EIS (electrochemical impedance spectroscopy) data show that polysulfides in the electrolyte solution play an important role for the stability of the interface on the lithium electrode. These results combined with SEM (scanning electron microscope) images show that the decomposition of the lithium salt (LiTFSI) on the lithium electrode can be prevented by a surface film formed with polysulfides. As shown by XPS (X-ray photoelectron spectroscopy) spectra and depth profiling, the surface film on the lithium anode cycled in the electrolyte solution with polysulfides can be assumed to be composed of two layers. The top layer is composed of the products of the decomposition of LiTFSI and the bottom layer is composed of lithium sulfide produced by the reaction between lithium metal and the polysulfides in the electrolyte solution. We suggest that the bottom layer efficiently prevents the decomposition of the lithium salt on the lithium anode in lithium–sulfur batteries, thereby increasing the stability and cyclability.

1. Introduction

With a steadily increasing demand for clean and efficient energy storage devices, lithium batteries have been continuously developed in the past decades [1–4]. Owe to their high specific energy (energy per unit weight) and energy density (energy per unit volume), lithium batteries are currently being applied as power sources for an increasing diversity of devices, from cars to microchips [5]. However, the highest energy storage the Li-ion batteries can deliver is not enough to meet the demands of key markets, such as electric vehicles [5]. To overcome this challenge, battery systems based on lithium anodes are receiving considerable interest [6,7]. Here the lithium–sulfur battery is one of those systems, due to its high theoretical energy density of about 2600 Wh kg^{-1}, assuming the complete reaction of sulfur with lithium to form Li_2S [6,8]. In addition, the lithium–sulfur battery has advantages such as natural abundance of key elements, low cost, and environmental friendliness [9,10]. However, rechargeable lithium–sulfur batteries suffer from capacity degradation upon cycling, which can be mainly attributed to the high solubility of the polysulfides, formed as reaction intermediates in the organic electrolyte solutions during the discharge–charge process [11–13]. The soluble polysulfides will result in a shuttle reaction, which will cause active material loss and an accelerated failure of the lithium anode [14,15]. Thus, a key challenge is to improve the stability of the lithium anode in a lithium–sulfur battery to realize the full potential of the technology [16,17].

However, most of the attempts to improve the property of lithium–sulfur batteries focus on the sulfur cathode and the

* Corresponding author.
E-mail addresses: sxiong@nudt.edu.cn, shizhao.xiong@hotmail.com (S. Xiong).

0378-7753/$ – see front matter © 2013 Elsevier B.V. All rights reserved.
http://dx.doi.org/10.1016/j.jpowsour.2013.02.072

electrolyte solution, whereas the lithium anode for lithium–sulfur batteries has not attracted enough attention [18–21]. In fact, the situation at the lithium anode in lithium–sulfur batteries is very different from those lithium electrodes studied before because of the unique electrolyte solution and the presence of soluble polysulfides [17,22].

On the basis of previous publications, a stable solid electrolyte interphase (SEI) plays a key role for the behavior of lithium anode. The thickness, morphology, composition, and compactness of the SEI all significantly affect battery performance [22–29]. The electrolyte solution, 1 M $LiN(CF_3SO_2)_2$ (LiTFSI) in 1,3-dioxolane (DIOX) and 1,2-dimethoxyethane (DME, 1:1, v/v) mixed solvents, has been widely used for lithium–sulfur batteries [30–34]. In the present work, the behavior and properties of the solid electrolyte interphase on the lithium anode cycled in an electrolyte solution for lithium–sulfur batteries has been studied using X-ray photoelectron spectroscopy (XPS), scanning electron microscope (SEM) and electrochemical impedance spectroscopy (EIS). Furthermore, the role of polysulfides on the formation and the behavior of the SEI in lithium–sulfur batteries are discussed in detail and the relationship between the SEI and lithium anode is introduced.

2. Experimental

Lithium metal foil (100 μm, Denway, China) was received and stored in an argon atmosphere glove box. The lithium disk was immersed in the electrolyte solutions (1 M LiTFSI/DIOX/DME (1:1, v/v). Solvents, analytically pure, water content $<3.0 \times 10^{-3}$%, Novolyte. LiTFSI, 99.95%, Aldrich) for 5 h to obtain the lithium sample without cycling. Meanwhile, lithium metal symmetrical coin cells were assembled in an argon atmosphere glove box to obtain the lithium samples after cycling. Each electrode was a 10 mm diameter lithium metal disk, and the separator was Celgard® 2500 (Celgard, 20 μm thick). Standard internal stainless steel spacers and springs provided internal pressure. A multichannel battery test system (LAND CT2001A) was used to cycle the symmetrical cells at a current density of 0.40 mA cm^{-2}. The cycling time was 30 min per cycle (15 min "charge" and 15 min "discharge"), approximately equal to plating and stripping 0.36 C cm^{-2} of lithium. After cycling the cell was disassembled to retrieve the anodes cycled in different electrolyte solutions. For further characterization, the anodes were washed with DME and further dried in an argon-filled glove box for 2 h at room temperature. Impedance spectroscopy analysis was performed using an Autolab Electrochemical Workstation (AUT71864) over a frequency range of 0.01 Hz–1 MHz and the perturbation amplitude was 5 mV.

The samples were transferred from the glove box to the SEM system (HTACHI S-4800) or the XPS systems (K-Alpha 1063, Thermo Fisher Scientific) without exposing them to atmospheric contaminants using the special transfer system described previously [35]. The X-ray photoelectron spectra were obtained by using Al-Kα radiation, operating at a power of 72 W (12 kV) with a base pressure of 10^{-9} Torr. The diameter of the analyzed area of the samples was 400 μm and an argon ion beam (accelerating voltage 3 keV, ion beam current 6 μA) was employed for the etching process.

For preparing sulfur cathode, 60 wt.% of sulfur (99.98%, Aldrich), 25 wt.% of acetylene black (Alfa) and 15 wt.% of PVdF (polyvinylidenefluoride) binder were taken in NMP (*N*-methyl-2-pyrrolidone) solvent, as described previously [35]. After that, the slurry was mixed in a spex ball mill at room temperature for 2.5 h at 580 rpm and coated on an aluminum current collector. Then the sulfur cathode was dried for 24 h at room temperature and further at 60 °C under vacuum for 12 h.

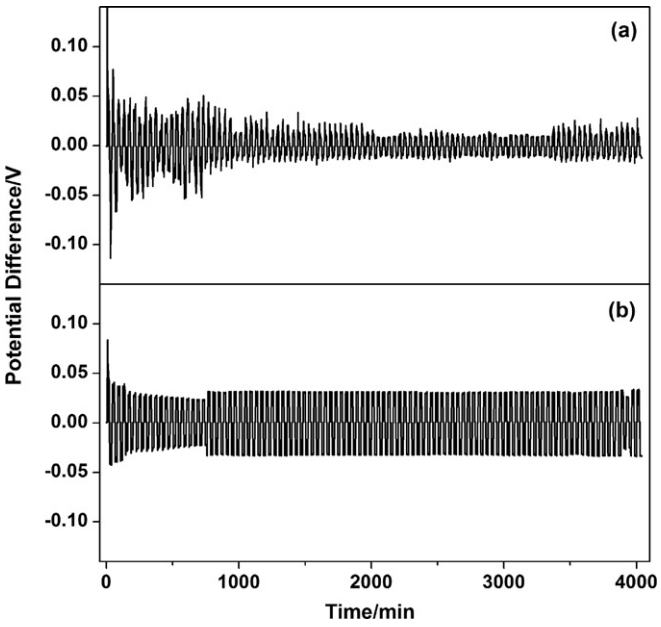

Fig. 1. Cycling behavior of a symmetrical cell with the electrolytes (a) 1 M LiTFSI/DIOX/DME (1:1, v/v) and (b) 0.8 M LiTFSI/0.2 M Li_2S_6/DIOX/DME (1:1, v/v).

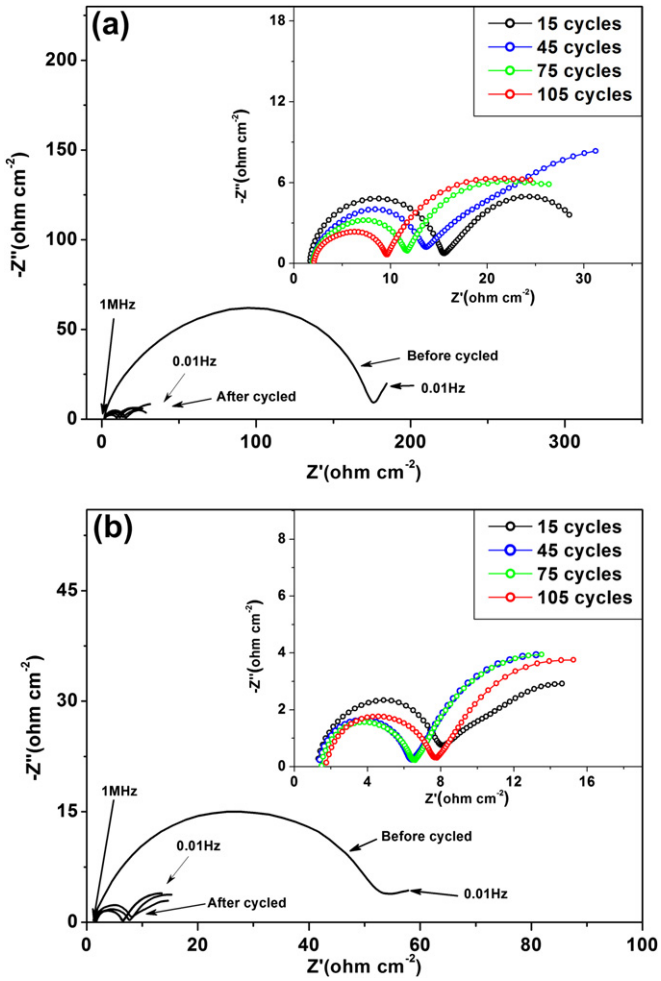

Fig. 2. Impedance plots from the symmetrical cell containing (a) 1 M LiTFSI/DIOX/DME (1:1, v/v) and (b) 0.8 M LiTFSI/0.2 M Li_2S_6/DIOX/DME (1:1, v/v). Inset: close up of the impedance plots from the cells after cycling.

3. Results and discussion

Lithium symmetrical cells have been widely used to study the formation of a SEI on lithium anodes [36,37]. The stability of the system is indicated by the changes of the potential over many cycles. The charge–discharge curves of the symmetrical cell cycled with 1 M LiTFSI/DIOX/DME (1:1, v/v) (Fig. 1(a)) show an irregular potential change during the whole period, which means that the system is unstable during cycling. As mentioned previously, the low degree of discharge will not disrupt the structure of the lithium electrode. Therefore, an unstable interface between the lithium electrode and the electrolyte solution is the most likely explanation for the irregular potential change. It suggests that there is a continuous reaction between the lithium electrode and the components of the electrolyte during cycling which leads to the unstable interface. As shown in Fig. 1(b), the charge–discharge curves of the symmetrical cell cycled with the electrolyte containing polysulfides show a different behavior. During the first 750 min cycling, the potential decreased slowly in order to maintain the constant current. After that the curves show a potential leveling until 4000 min, indicating that a stable surface film is formed on the lithium electrode. It suggests that the presence of polysulfides reduces the reaction between the lithium electrode and the components of the electrolyte solution.

To further investigate the formation and stability of the interface between the electrolyte solution and the lithium electrode during cycling, electrochemical impedance spectra (EIS) were measured. The main contribution to the resistance of the lithium electrodes before cycling is from the transfer of lithium ion across the surface film [35,38,39]. Compared to the lithium electrode immersed in 1 M LiTFSI/DIOX/DME (1:1, v/v), the resistance value of the lithium electrode in the electrolyte solution with polysulfides is much lower. This suggests that polysulfides play an important role in the formation of the surface film on the lithium electrode, as discussed previously in literature [35]. However, the impedance behavior of lithium electrodes after cycling shows a different feature. Each impedance spectrum has two semicircles, relating to the Li-ion migration through the surface film on the lithium anode (high frequency semicircle) and the charge transfer across the interface (low frequency semicircle) respectively [40–43]. As shown in Fig. 2(a), the resistance relating to the ionic conductivity of the surface film decreases with increasing cycle number in 1 M LiTFSI/DIOX/DME (1:1, v/v). This indicates that the interface between the lithium electrode and the electrolyte solution is unstable during cycling. However, the corresponding resistance when cycling with the electrolyte containing polysulfides also decreases during initial cycling and then stabilizes after 45 cycles. It suggests that the surface film on the lithium electrode stabilizes after a certain

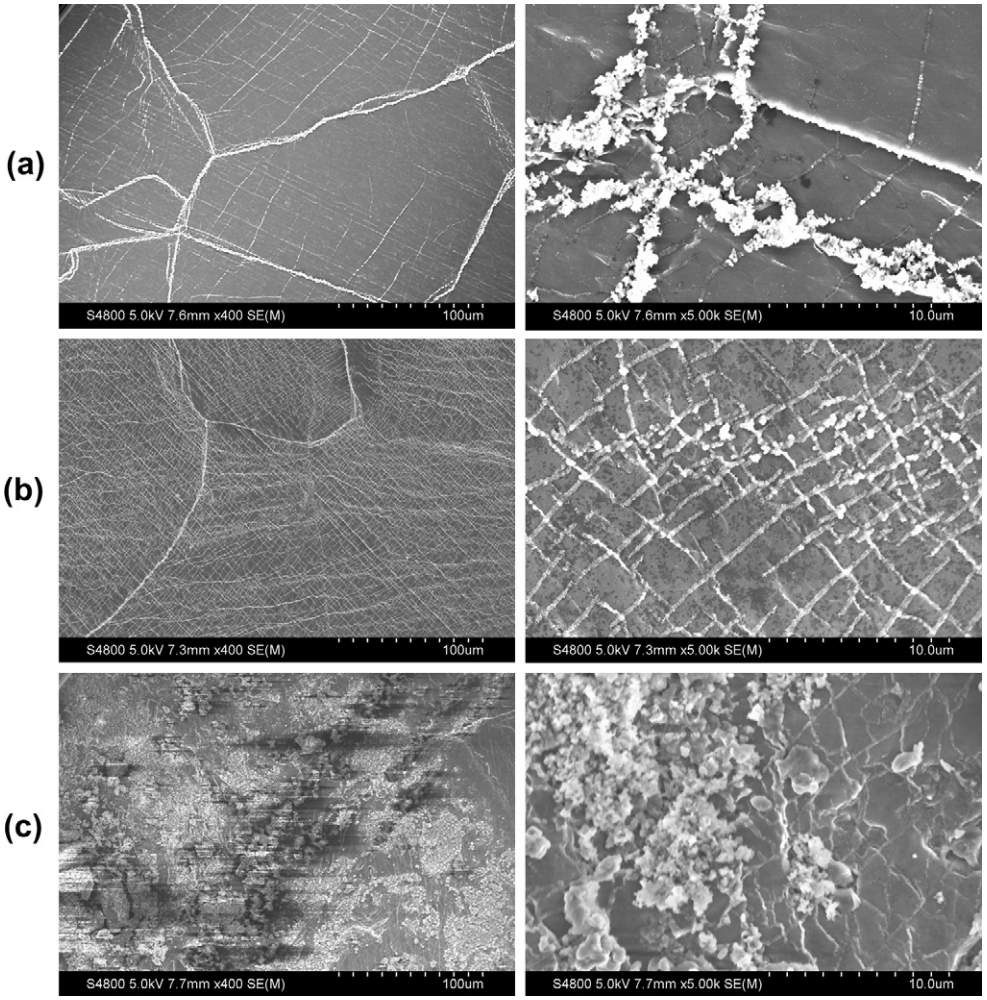

Fig. 3. SEM images of lithium anodes (a) immersed in 1 M LiTFSI/DIOX/DME (1:1, v/v) for 5 h, cycled for (b) a cycle and (c) 20 cycles. Left column: low magnification, right column: high magnification.

number of cycles. However, after 105 cycles the resistance value increases, demonstrating the disruption of the surface film, as discussed above.

To understand the behavior of the interface with cycling, the morphology of the surface film on the lithium electrodes were investigated using scanning electron microscopy. As shown in Fig. 3(a), the reaction between lithium metal and electrolyte solution results in deposits on the surface film along the line cracks, after the electrode has been immersed in 1 M LiTFSI/DIOX/DME (1:1, v/v) for 5 h. The line cracks are also present on the native lithium metal [35]. This indicates that the components of the electrolyte penetrate through the native surface film to react with the lithium metal. After cycling more line cracks are visible on the surface film (Fig. 3(b)), with deposits along the line cracks, demonstrating the reaction during the cycling process. A surface film densely covered with line cracks could be unstable during the repeating lithium deposition–dissolution process, resulting in the irregular potential change in Fig. 1(a). After 20 cycles the lithium electrode (Fig. 3(c)) is completely covered with deposits. In contrast, on the surface film of the electrode (Fig. 4(b)) cycled with 0.8 M LiTFSI/0.2 M Li_2S_6/DIOX/DME (1:1, v/v) very little deposits are found even after 20 cycles. As shown in Fig. 4(a), the line cracks on the lithium sample as received remain after the first cycle in the electrolyte solution. The images with high magnification show that there are some deposits on the lithium electrode after 20 cycles, but the surface film is still unbroken and compact. The above data suggest that the reaction between the lithium electrode and electrolyte solution has been prevented by the interface formed in contact with the electrolyte containing polysulfides.

To understand the special structure of the surface film on the lithium electrode after cycling in the electrolyte containing polysulfides, chemical composition and depth profile information of the surface film were obtained by X-ray photoelectron microscopy spectra (XPS). As shown in Fig. 5, the chemical composition of the top layer (0–30 s) is very different from the bottom layer (330–1830 s) of the surface film. In the top layer, the peaks in the O1s spectra can be attributed to Li_2CO_3 (531.1 eV), Li_2SO_3 (531.8 eV) and Li_2O (528.3 eV) [14,29,44]. For the S2p and the F1s spectra, the peaks are attributed to products of LiTFSI decomposition on the lithium electrode, such as $Li_2S_2O_3$ (163.1 eV), $-NSO_2CF_3$ (169.0 eV), Li_3N (398.6 eV) and LiF (684.8 eV) [14,29,44–48]. Under the top layer, the peaks in the S2p spectra can be attributed to Li_2S (160.1 eV) and Li_2S_2 (161.2 eV), produced by the reaction between high-order polysulfides and the lithium anode [14]. For the O1s and F1s spectra, Li_2O in the surface film may originate from the native film and lithium salt decomposition and the LiF may originate from the reaction with HF, which is produced by the $TFSI^-$ decomposition and can diffuse into the film very easily. These results suggest

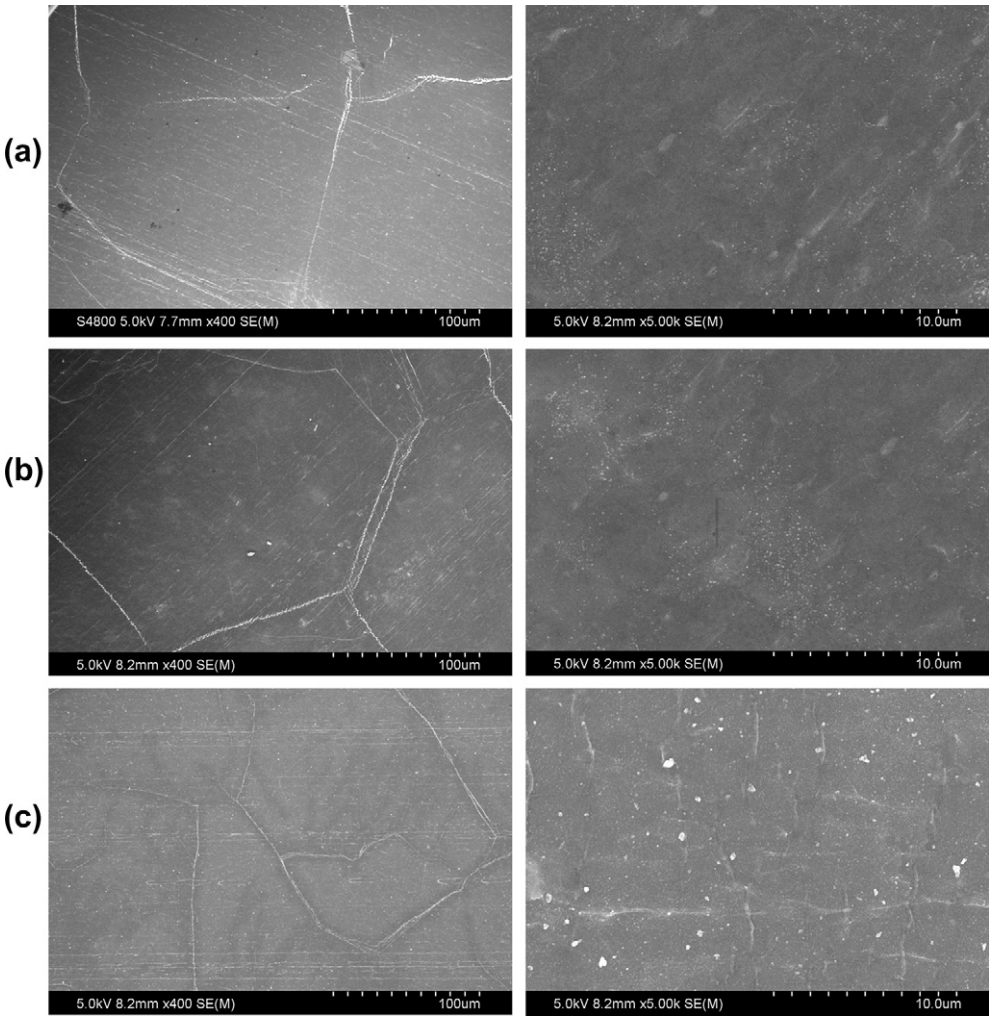

Fig. 4. SEM images of the lithium anode (a) immersed in 0.8 M LiTFSI/0.2 M Li_2S_6/DIOX/DME (1:1, v/v) for 5 h, cycled for (b) a cycle and (c) 20 cycles. Left column: low magnification, right column: high magnification.

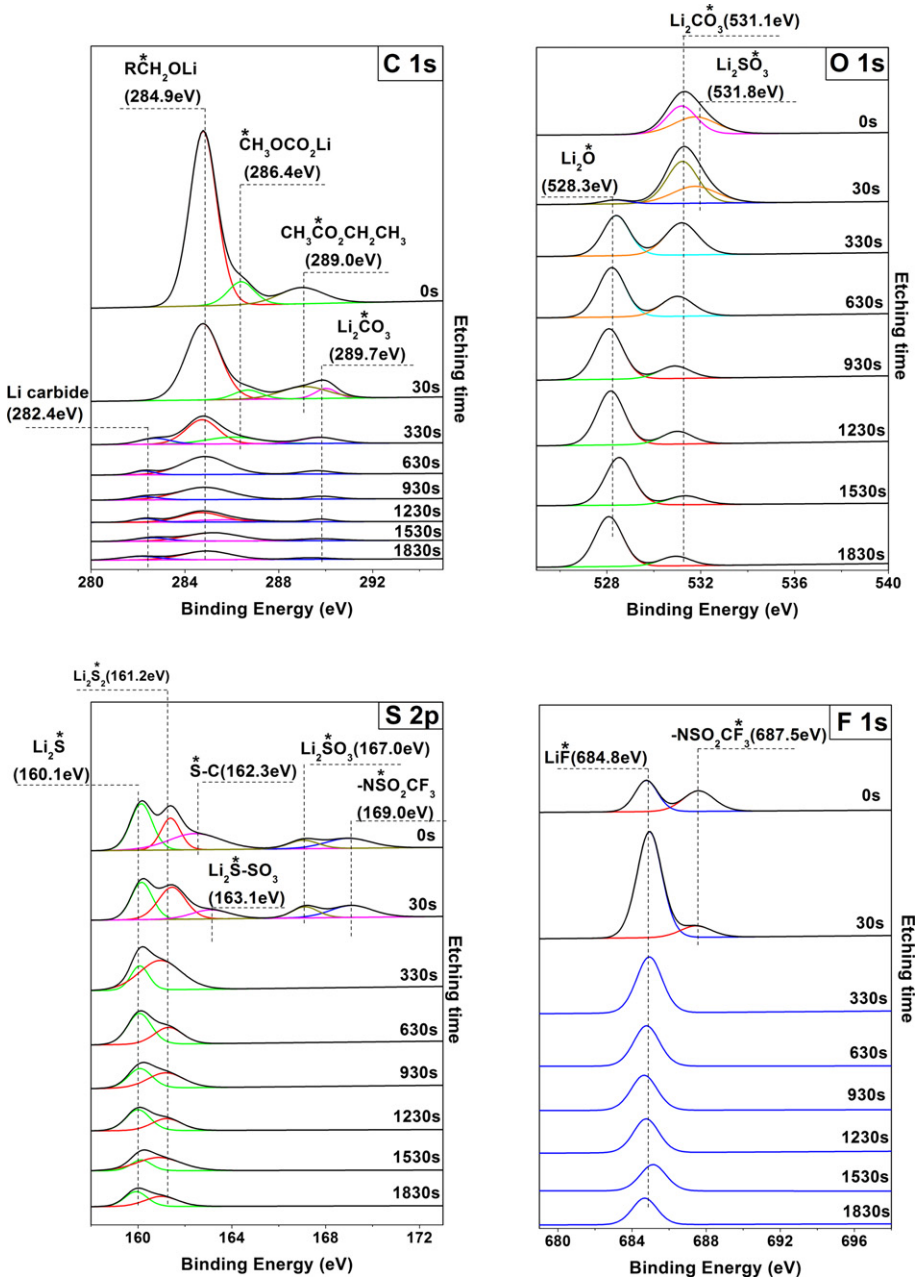

Fig. 5. X-ray photoelectron microscopy (XPS) spectra from the lithium anode cycled in 0.8 M LiTFSI/0.2 M Li_2S_6/DIOX/DME (1:1, v/v) for 20 cycles.

that the decomposition of LiTFSI on the lithium electrode is prevented by the bottom layer consisting of lithium sulfides. However, the presence of Li_2CO_3, and RCH_2OLi (284.9 eV) throughout the film shows that the decomposition of solvents cannot be prevented by this layer.

The chemical composition distribution is demonstrated by the depth profiles of each element in the surface film. As shown in Fig. 6, the S and F concentration in the top layer is considerably higher than that in the bottom layer. This demonstrates that most of the products of LiTFSI decomposition are distributed in the top layer. In the bottom layer, the concentration of sulfur is constant. Thus, the surface film of the lithium anode cycled in the electrolyte solution with polysulfides can be divided into two sub layers. The top layer is composed of the products of LiTFSI decomposition and the bottom layer is composed of lithium sulfide produced by the reaction with the polysulfides in the electrolyte. This indicates that the bottom layer plays an important role to prevent the decomposition of LiTFSI. This interface, with the special structure, results in a stable potential during the charge–discharge cycles, as discussed for Fig. 1. However, the surface film cannot prevent the shuttle phenomenon in lithium–sulfur batteries, which results in capacity loss and low columbic efficiency of the battery's system [14,15,17,35] because the reaction between polysulfides and the lithium anode will be active on the interface.

On the basis of the above data, we can understand the behavior of the surface film on lithium anode in lithium–sulfur batteries with 1 M LiTFSI/DIOX/DME (1:1, v/v) as the electrolyte solution during the charge–discharge process of the battery. As shown in Fig. 7, the discharge process of lithium–sulfur batteries can be divided into two plateaus. The high plateau (2.4–2.1 V) corresponds

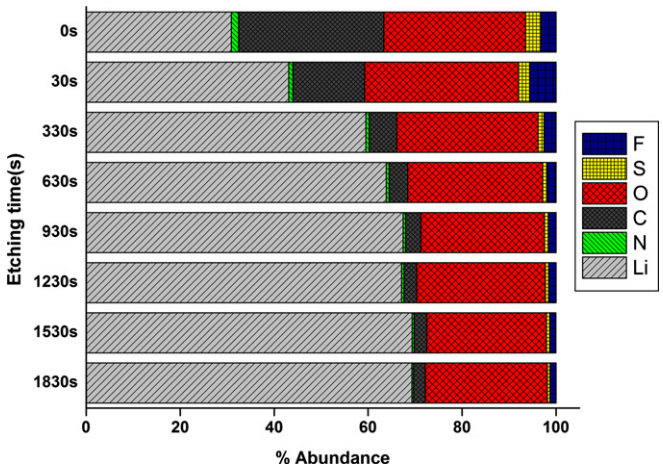

Fig. 6. Depth profile for the lithium anode surface cycled in 0.8 M LiTFSI/0.2 M Li_2S_6/DIOX/DME (1:1, v/v) for 20 cycles.

to the reduction of elemental sulfur at the cathode to form soluble high-order polysulfides. S_6^{2-} and S_8^{2-} are the main types of polysulfides in the electrolyte solution at this stage [5,10,11]. The high-order polysulfides will migrate through the separator to the surface of the lithium electrode, as shown on the left of Fig. 7. On the basis of the previous data, the top layer of the surface film is rather thin (only 30 s etching) and the surface film is densely covered by line cracks. Hence, the high-order polysulfides will penetrate through the surface film to react with the lithium metal. Solid precipitates (lithium sulfide, Li_2S or/and Li_2S_2) depositing on the lithium electrode and soluble low-order polysulfides (mainly S_3^{2-}, S_4^{2-}) are produced at the same time. The thickness of the bottom layer, which consists of lithium sulfide, will continuously increase during the first part of the discharge process. The low plateau (2.1–1.5 V) corresponds to the reduction of low-order polysulfides to form a solid Li_2S film on the carbon framework of the cathode [11]. In fact the reactivity of low-order polysulfides with lithium metal is much lower than that of higher order polysulfides [15]. In addition, the bottom layer would be thick enough to prevent the reaction between the lithium metal and electrolyte solution, as shown in the middle column of Fig. 7.

The charge process shows a different picture of the behavior of the surface film. With the continuous oxidation of low-order polysulfides on the cathode, the concentration of high-order polysulfides increases to a rather high level when the battery system is charged to 2.3 V [15,49]. After that the reaction between high-order polysulfides and the solid lithium sulfide on lithium electrode is so active that it uses up the high-order polysulfides migrating from the cathode, leading to the shuttle phenomenon. The low-order polysulfides produced by the reaction on the lithium anode diffuse back to the cathode and generate high-order polysulfides again. The continuous cycling results in the voltage leveling of the charge curve. As shown in the schematic representation in Fig. 7, the top layer covering the solid lithium sulfide could potentially prevent the shuttle, by blocking the contact between high-order polysulfides in the electrolyte solution and lithium sulfides in the bottom layer of the surface film.

4. Conclusions

To understand the behavior of the solid electrolyte interphase on the lithium electrode during cycling in lithium–sulfur batteries, the morphology, chemical composition and depth profile of the surface film were studied for two different electrolyte solutions using X-ray photoelectron spectroscopy (XPS), scanning electron microscope (SEM) and electrochemical impedance spectroscopy (EIS). As shown in discharge–charge curves and EIS spectra, the symmetrical cell cycled in the electrolyte solution with polysulfides results in a stable potential, which means the system has a stable interface between the lithium electrode and the electrolyte solution. Furthermore, SEM images show that the decomposition of lithium salt on the lithium electrode can be prevented by the surface film formed with polysulfides, which is attributed to the

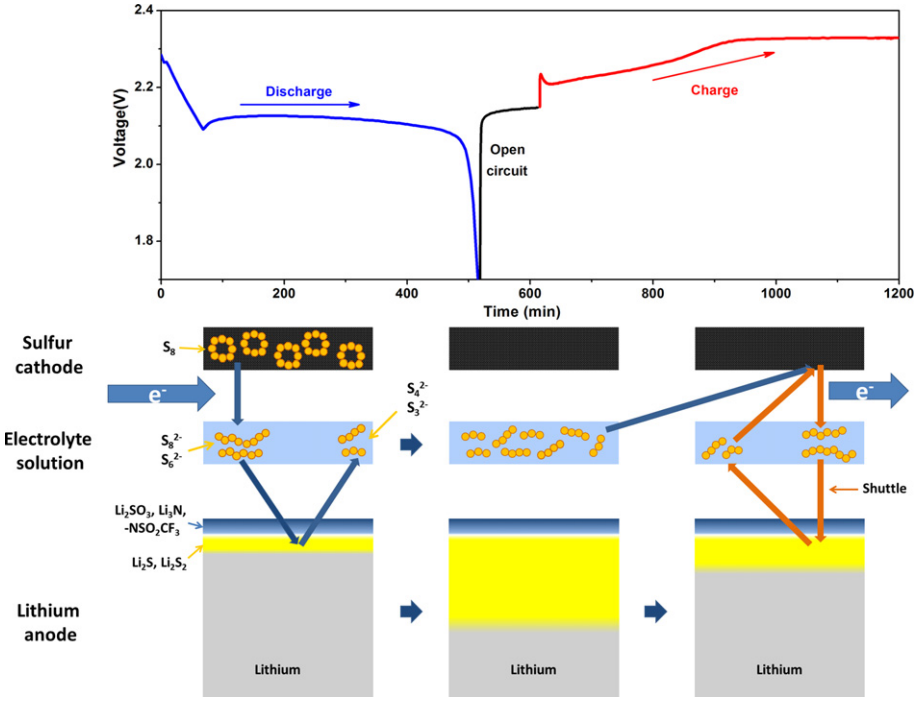

Fig. 7. Schematic representation of the surface film behavior on the lithium anode in a lithium–sulfur battery cycled with 0.8 M LiTFSI/0.2 M Li_2S_6/DIOX/DME (1:1, v/v).

special structure of the film. On the basis of the XPS spectra and depth profiling, the surface film can be assumed to be formed of two sub layers with the top layer composed of the products of electrolyte solution decomposition and the bottom layer composed of lithium sulfide. We suppose that the bottom layer plays an important role to prevent decomposition of LiTFSI. On the basis of the above discussion, the top layer and the bottom layer of the surface film play different roles on the behavior of the lithium electrode.

Acknowledgements

We are grateful to the support of the aid program for the Science and Technology Innovative Research Team in Higher Educational Institutions of Hunan Province. The authors thank Per Jacobsson, Aleksandar Matic and Andrew Poole for their valuable discussions and input to the work.

References

[1] H. Wang, Y. Yang, Y. Liang, J.T. Robinson, Y. Li, A. Jackson, Y. Cui, H. Dai, Nano Lett. 11 (2011) 2644.
[2] Y. Yang, M.T. McDowell, A. Jackson, J.J. Cha, S.S. Hong, Y. Cui, Nano Lett. 10 (2010) 1486.
[3] M. Armand, J.M. Tarascon, Nature 451 (2008) 652.
[4] X. Ji, K.T. Lee, L.F. Nazar, Nat. Mater. 2460 (2009) 500.
[5] P.G. Bruce, S.A. Freunberger, L.J. Hardwick, J.-M. Tarascon, Nat. Mater. 11 (2012) 19.
[6] J. Hassoun, B. Scrosati, Adv. Mater. 22 (2010) 5198.
[7] S.A. Freunberger, Y. Chen, Z. Peng, J.M. Griffin, L.J. Hardwick, F. Barde, P. Novak, P.G. Bruce, J. Am. Chem. Soc. 133 (2011) 8040.
[8] Y. Yang, G. Yu, J.J. Cha, H. Wu, M. Vosgueritchian, Y. Yao, Z. Bao, Y. Cui, ACS Nano 5 (2011) 9187.
[9] R. Elazari, G. Salitra, A. Garsuch, A. Panchenko, D. Aurbach, Adv. Mater. 23 (2011) 5641.
[10] C. Barchasz, F. Molton, C. Duboc, J.-C. Lepretre, S. Patoux, F. Alloin, Anal. Chem. 84 (2012) 3973.
[11] S.E. Cheon, K.S. Ko, J.H. Cho, S.W. Kim, E.Y. Chin, J. Electrochem. Soc. 150 (2003) A796.
[12] S.E. Cheon, K.S. Ko, J.H. Cho, S.W. Kim, E.Y. Chin, J. Electrochem. Soc. 150 (2003) A800.
[13] E. Peled, Y. Sternberg, A. Gorenshtein, Y. Lavi, J. Electrochem. Soc. 136 (1989) 1621.
[14] D. Aurbach, E. Pollak, R. Elazari, G. Salitra, C.S. Kelley, J. Affinitob, J. Electrochem. Soc. 156 (2009) A694.
[15] Y.V. Mikhaylik, J.R. Akridge, J. Electrochem. Soc. 151 (2004) A1969.
[16] Y.M. Lee, N.S. Choi, J.H. Park, J.K. Park, J. Power Sources 119 (2003) 964.
[17] X. Liang, Z. Wen, Y. Liu, M. Wu, J. Jin, H. Zhang, X. Wu, J. Power Sources 196 (2011) 9839.
[18] J. Schuster, G. He, B. Mandlmeier, T. Yim, K.T. Lee, T. Bein, L.F. Nazar, Angew. Chem. Int. Ed. 51 (2011) 3591.
[19] G.-C. Li, G.-R. Li, S.-H. Ye, X.-P. Gao, Adv. Energy Mater. 2 (2012) 1238.
[20] J. Kim, D.-J. Lee, H.-G. Jung, Y.-K. Sun, J. Hassoun, B. Scrosati, Adv. Funct. Mater. (2012), http://dx.doi.org/10.1002/adfm.201200689.
[21] J. Wang, j. Yang, C. Wan, K. Du, J. Xie, N. Xu, Adv. Energy Mater. 13 (2003) 487.
[22] Y.V. Mikhaylik, U.S. Patent, 2004, 6706449.
[23] P.B. Balbuena, Y. Wang, Lithium-Ion Batteries Solid-Electrolyte Interphase, Imperial College Press, London, 2004.
[24] T.A. Skotheim, U.S. Patent, 2004, 6733924.
[25] T.A. Skotheim, U.S. Patent, 2007, 7247408.
[26] D. Aurbach, M.L. Daroux, P.W. Faguy, E. Yeager, J. Electrochem. Soc. 135 (1988) 1863.
[27] D. Aurbach, E. Zinigrad, H. Teller, Y. Cohen, G. Salitra, H. Yamin, P. Dan, E. Elsterb, J. Electrochem. Soc. 149 (2002) A1267.
[28] E. Zinigrad, E. Levi, H. Teller, G. Salitra, D. Aurbach, P. Dan, J. Electrochem. Soc. 151 (2004) A111.
[29] D. Aurbach, I. Weissman, A. Schechter, Langmuir 12 (1996) 3991.
[30] Y. Fu, A. Manthiram, Chem. Mater. 24 (2012) 3081.
[31] C. Liang, N.J. Dudney, J.Y. Howe, Chem. Mater. 21 (2009) 4724.
[32] J. Nelson, S. Misra, Y. Yang, A. Jackson, Y. Liu, H. Wang, H. Dai, J.C. Andrews, Y. Cui, M.F. Toney, J. Am. Chem. Soc. 134 (2012) 6337.
[33] X. Li, Y. Cao, W. Qi, L.V. Saraf, J. Xiao, Z. Nie, J. Mietek, J.-G. Zhang, B. Schwenzer, J. Liu, J. Mater. Chem. 21 (2011) 16603.
[34] M. Hagen, S. Dörfler, H. Althues, J. Tübke, M.J. Hoffmann, S. Kaskel, K. Pinkwart, J. Power Sources 213 (2012) 239.
[35] S. Xiong, K. Xie, Y. Diao, X. Hong, Electrochim. Acta 83 (2012) 78.
[36] G.H. Lane, A.S. Best, D.R. MacFarlane, M. Forsyth, A.F. Hollenkamp, Electrochim. Acta 55 (2010) 2210.
[37] J.-K. Kima, A. Matica, J.-H. Ahnb, P. Jacobsson, J. Power Sources 195 (2010) 7639.
[38] M.A. Vorotyntsev, M.D. Levi, A. Schechter, D. Aurbach, J. Phys. Chem. B 105 (2001) 188.
[39] A. Zaban, E. Zinigrad, D. Aurbach, J. Phys. Chem. C 100 (1996) 3089.
[40] D. Aurbach, K. Gamolsky, B. Markovsky, Y. Gofer, M. Schmidt, U. Heider, Electrochim. Acta 47 (2002) 1423.
[41] J.G. Thevenin, R.H. Muller, J. Electrochem. Soc. 134 (1987) 273.
[42] J.G. Thevenin, R.H. Muller, J. Electrochem. Soc. 134 (1987) 2650.
[43] D. Aurbach, M.D. Levi, E. Levi, H. Telier, B. Markovsky, G. Salitra, J. Electrochem. Soc. 145 (1998) 3024.
[44] A. Schechter, D. Aurbach, Langmuir 15 (1999) 3334.
[45] S. Shiraishi, K. Kanamura, Z.-i. Takehara, Langmuir 13 (1997) 3542.
[46] H. Ota, Y. Sakata, X. Wang, J. Sasahara, E. Yasukawa, J. Electrochem. Soc. 151 (2004) A437.
[47] I. Ismail, A. Noda, A. Nishimoto, M. Watanabe, Electrochim. Acta 46 (2001) 1595.
[48] K. Kanamura, H. Tamura, S. Shiraishi, Z. Takehara, Electrochim. Acta 40 (1995) 913.
[49] K. Kumaresan, Y.V. Mikhaylik, R.E. White, J. Electrochem. Soc. 155 (2008) A576.